



An experimental evaluation of the use of $\Delta^{13}\text{C}$ as a proxy for palaeoatmospheric CO_2

Barry H. Lomax^{a,*}, Janice A. Lake^b, Melanie J. Leng^{c,a}, Phillip E. Jardine^d

^a *The School of Biosciences, Division of Agricultural and Environmental Sciences, The University of Nottingham, Sutton Bonington Campus, Sutton Bonington, Leicestershire LE12 5RD, UK*

^b *Department of Animal and Plant Sciences, University of Sheffield, Sheffield S10 2TN, UK*

^c *Centre for Environmental Geochemistry, British Geological Survey, Keyworth, Nottingham NG12 5GG, UK*

^d *Institute of Geology and Palaeontology, University of Münster, 48149 Münster, Germany*

Received 26 April 2018; accepted in revised form 18 December 2018; Available online 27 December 2018

Abstract

Understanding changes in atmospheric CO_2 over geological time via the development of well constrained and tested proxies is of increasing importance within the Earth sciences. Recently a new proxy (identified as the C3 proxy) has been proposed that is based on the relationship between CO_2 and carbon isotope discrimination ($\Delta^{13}\text{C}$) of plant leaf tissue. Initial work suggests that this proxy has the capacity to deliver accurate and potentially precise palaeo- CO_2 reconstructions through geological time since the origins of vascular plants (~ 450 Mya). However, the proposed model has yet to be fully validated through independent experiments. Using the model plant *Arabidopsis thaliana* exposed to different watering regimes and grown over a wide range of CO_2 concentrations (380, 400, 760, 1000, 1200, 1500, 2000 and 3000 ppm) relevant to plant evolution we provide an experimental framework that allows for such validation. Our experiments show that a wide variation in $\Delta^{13}\text{C}$ as a function of water availability is independent of CO_2 treatment. Validation of the C3 proxy was undertaken by comparing growth CO_2 to estimates of CO_2 derived from $\Delta^{13}\text{C}$. Our results show significant differences between predicted and observed CO_2 across all CO_2 treatments and water availabilities, with a strong under prediction of CO_2 in experiments designed to simulate Cenozoic and Mesozoic atmospheric conditions (≥ 1500 ppm). Further assessment of $\Delta^{13}\text{C}$ to predict CO_2 was undertaken using Monte Carlo error propagation. This suite of analysis revealed a lack of convergence between predicted and observed CO_2 . Collectively these findings suggest that the relationship between $\Delta^{13}\text{C}$ and CO_2 is poorly constrained. Consequently the use of $\Delta^{13}\text{C}$ as a proxy to reconstruct palaeoatmospheric CO_2 is of limited use as the estimates of CO_2 are not accurate when compared to known growth conditions.

© 2019 The Authors. Published by Elsevier Ltd. This is an open access article under the CC BY license (<http://creativecommons.org/licenses/by/4.0/>).

Keywords: Water-use efficiency; Carbon isotope; Discrimination; Atmospheric CO_2 concentration

1. INTRODUCTION

Understanding both the long term carbon cycle and rapid perturbations in atmospheric CO_2 observed through the geological record has become an increasingly important area of scientific enquiry. A major limiting step in

understanding the climate system sensitivity to changes in atmospheric CO_2 over geological time has been the variability in modelled solutions of palaeo- CO_2 concentration which vary considerably both between (GEOCARB *vs* COPSE (Bernier and Kothavala, 2001; Bergman et al., 2004)) and within model families (GEOCARB III *vs* GEOCARBSULF (Bernier and Kothavala, 2001; Bernier, 2006)). For example within the GEOCARB suite of models comparisons between GEOCARB III and GEOCARBSULF

* Corresponding author.

E-mail address: Barry.lomax@nottingham.ac.uk (B.H. Lomax).

suggests modelled values ranging from ~ 3400 ppm in the Early Triassic to ~ 500 ppm in the Late Triassic. To constrain these models and evaluate refinements made through model development requires the development of mechanistically based CO_2 proxies that have been independently tested and fully validated (Lomax and Fraser, 2015).

Recent work on proxy development (Franks et al., 2014) has led to the suggestion that CO_2 concentrations may have been substantially lower than previous reconstruction and modelling studies have indicated. Franks et al. (2014) suggested that large long-term CO_2 perturbations (~ 2000 – 3000 ppm) are unlikely and that over geological long-term CO_2 may have been <1000 ppm since the evolution and radiation of forests in the Middle Devonian (Morris et al., 2015). Their data compare favourably to modelled solutions of the long-term carbon cycle (Berner, 2006; Royer et al., 2014) and the temporally and spatially limited proxy record generated from the carbon isotope ($\delta^{13}\text{C}$) analysis of fossil liverworts (Fletcher et al., 2008). However the evaluation sensitivity analysis of the Franks et al. (2014) model as conducted by McElwain et al. (2016) suggests an alternative interpretation under which Phanerozoic CO_2 concentrations may have regularly exceeded 1000 ppm. However, the sensitivity analysis of McElwain et al. (2016) was subsequently critiqued by Franks and Royer (2017) and subsequently rebutted (McElwain et al. (2017)). More recently, Foster et al. (2017) compiled a series of CO_2 estimates from the literature (see SOM of Foster et al. (2017) for full details) via integrating five independent methods (stomata, pedogenic $\delta^{13}\text{C}$, liverwort $\delta^{13}\text{C}$, foraminiferal $\delta^{11}\text{B}$ and alkenone $\delta^{13}\text{C}$) to produce a LOESS CO_2 curve for the last 420 million years. This compiled LOESS CO_2 curve indicates that atmospheric CO_2 concentrations are lower than GEOCARB predications and partially supports the predictions of the Franks et al. (2014) model that CO_2 has remained below 1000 ppm for sustained periods during the Phanerozoic. In the compilation of Foster et al. (2017) CO_2 remains above 1000 ppm for most of the Triassic and the Early Jurassic (Anisian–Sinemurian) suggesting support for the sensitivity analysis of McElwain et al. (2016).

Recently a new proxy method has been developed based on $\delta^{13}\text{C}$ composition of C3 plant material and discrimination ($\Delta^{13}\text{C}$) with changes in $\Delta^{13}\text{C}$ being used as a basis to reconstruct $p\text{CO}_2$ (Schubert and Jahren, 2012). Following a full statistical analysis and quantification of uncertainty (Cui and Schubert, 2016) this method has recently been used to estimate changes in CO_2 through Cenozoic hyperthermals (Cui and Schubert, 2017) and to reconstruct atmospheric CO_2 through the Cretaceous (Barral et al., 2017). These results suggest atmospheric CO_2 could be lower than previously thought with particularly low CO_2 estimates for the middle Cretaceous. However these data plot outside of the 95% confidence limits of the Foster et al. (2017) study (Fig. 1) and are at odds with stomatal based estimates of CO_2 through OAE 1d (Richey et al., 2018) and OAE 2 (Barclay et al., 2010). Most recently Schubert and Jahren (2018) have focused on assessing the effects of photorespiration on $\Delta^{13}\text{C}$ and thus the C3 proxy through a round of experiments growing *Arabidopsis thaliana* over a range of

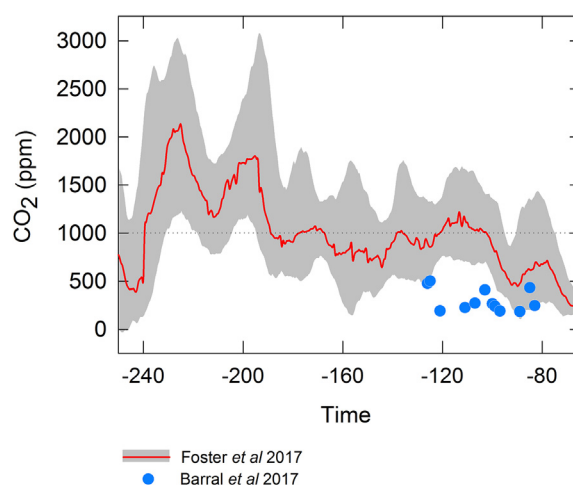


Fig. 1. Modelled and predicted values of atmospheric CO_2 over geological time. Blue circles are from Barral et al. (2017) reconstructed following the methods of Schubert and Jahren (2012) and Cui and Schubert (2016). The red line is the LOESS CO_2 curve of Foster et al. (2017) and the grey shading is the 95% confidence limit of their CO_2 prediction. (For interpretation of the references to colour in this figure legend, the reader is referred to the web version of this article.)

sub-ambient CO_2 concentrations. These data were then combined with pre-existing datasets (Schubert and Jahren, 2018) to investigate this relationship at 12 different CO_2 concentrations spanning 97 ppm through to 2255 ppm. They conclude that a $\sim 3.5\%$ change in $\Delta^{13}\text{C}$ can be prescribed to an increase in CO_2 from ~ 100 to 2250 ppm and that change in discrimination is independent of C_i/C_a (ratio of internal CO_2 to external CO_2). However, this independence was not tested for (experimentally) within their system.

If the use of $\Delta^{13}\text{C}$ could be independently validated it would offer a major new resource for the palaeoclimate community as C3 vascular plants are thought to originate in the Upper Ordovician (Middle Katian) (Stemans et al., 2009). This would be of particular importance as more CO_2 predictions for the Lower Palaeozoic are urgently required. Clearly the development of a well constrained proxy that could be used to deliver a large number of estimates of CO_2 through this time interval and further back to the origin of vascular plants would be a major advance in the understanding of the Earth system.

From an ecophysiological standpoint changes in $\Delta^{13}\text{C}$ are linked to changes in water use efficiency (WUE) of the plants that are ultimately controlled by the opening and closure of the stomatal pore complex which regulates gas exchange. For $\Delta^{13}\text{C}$ to be used as an accurate and precise method to reconstruct $p\text{CO}_2$ the major requirement is to demonstrate that changes in CO_2 are the main driver of changes in $\Delta^{13}\text{C}$. Further this needs to be independent of other environmental conditions that can alter C_i/C_a which in turn influence WUE . Factors that can influence C_i/C_a include but are not limited to irradiance (Ehleringer et al., 1986), temperature (Körner et al., 1991), salinity (Guy et al., 1980) and logically the amount of water availability (Farquhar et al., 1980; Kohn, 2010). Diefendorf et al.

(2010) reported a wide spread in $\delta^{13}\text{C}$ over a range of environments and in a recent review Cernusak et al. (2013) highlighted that there is an inherent tension between viewing $\Delta^{13}\text{C}$ as a sensor that responds to environmental cues or as a species specific set point driven by internal physiological constraints. This is further demonstrated by the ongoing scientific debate that is trying to establish what isotopically derived calculations of C_i/C_a are a measure of and how closely they relate to carbon draw down (C_i) (e.g., Seibt et al., 2008; Cernusak et al., 2009). The $\delta^{13}\text{C}$ of plant tissue ($\delta^{13}\text{C}_p$) can also vary considerably within a plant canopy with variation of $\sim 6\%$ being recorded from the base to the top of single *Fagus sylvatica* (beech) tree (Schleser, 1990). Over printed on this environmentally driven variability are differences in isotopic composition due to discrimination associated with tissue type reviewed in Gröcke (2002).

The fossil record acts as a strong filter. Therefore if carbon from bulk organic matter is analysed to generate $\Delta^{13}\text{C}$ it can be derived from different plant tissue and from plants from across a wide environmental gradient. It has previously been suggested that this filtering generates a smoothed average which might mitigate for these effects when using the $\delta^{13}\text{C}_p$ to predict the isotopic composition of CO_2 in air ($\delta^{13}\text{C}_a$) (Jahren and Arens, 2009). However, when tested experimentally using a sampling strategy designed to represent an allochthonous deposit this assertion was not supported, as large differences between predicted and measured $\delta^{13}\text{C}_a$ were observed (Lomax et al., 2012). Despite the finding of Lomax et al. (2012) the time averaging effect of the fossil record has again been suggested as a factor which has the capacity to mitigate and dampen other environmental signals (Schubert and Jahren, 2012), again without testing this assertion in an experimental framework. These issues might be particularly acute in periods of large scale carbon cycle and climate perturbations. As these events have the capacity to reshape standing terrestrial biomass via altering plant ecophysiological performance and by initiating floral overturn both factors that can influence plant $\Delta^{13}\text{C}$. These changes would then alter the isotopic composition of terrestrial organic matter in a manner that is potentially independent of changes in $p\text{CO}_2$.

More broadly and looking outside of the work that seeks to use $\Delta^{13}\text{C}$ as a method to reconstruct $p\text{CO}_2$, the nature of the relationship between $\delta^{13}\text{C}_p$, $\delta^{13}\text{C}_a$ and CO_2 in experimental systems needs to be clarified and responses tested (Lomax et al., 2012; Porter et al., 2017). Within all experimental systems to date, $\delta^{13}\text{C}_a$ becomes very negative when compared to the $\delta^{13}\text{C}$ of natural atmospheric CO_2 . Currently it is unknown if the models developed to explore carbon isotope fractionation at natural $\delta^{13}\text{C}_a$ values can be used when the value of the isotopic substrate is much more negative (compare ambient values of $\sim -8.0\%$ to experimental values that exceed $\sim -30\%$). Furthermore over geological time the $\delta^{13}\text{C}_a$ signature of CO_2 is known to be well constrained varying only slightly over the long-term, with short duration negative spikes shifting background values by $\sim 2\%$. There is also an issue of auto correlation between atmospheric CO_2 and $\delta^{13}\text{C}_a$ making inferences about any

perceived relationship difficult to disentangle (Lomax et al., 2012; Porter et al., 2017).

Consequently prior to the widespread deployment of such a novel proxy there is the requirement for rigorous experimental assessment of how other environmental factors impinge on the predictive capability of $\Delta^{13}\text{C}$ to be used as a proxy to predict $p\text{CO}_2$. Although Schubert and Jahren (2018) explicitly rule out changes in C_i/C_a being required to drive changes in $\Delta^{13}\text{C}$ this assumption was not tested for as water availability was controlled. Here we test one of the most important factors associated with C_i/C_a , namely water availability and how this factor influences $\Delta^{13}\text{C}$ generated from leaf tissue. We then use this dataset to test the utility of the proxy to predict $p\text{CO}_2$. As a first step to look at the validity of using isotope models constrained on ambient values of $\delta^{13}\text{C}_a$ we use an astomatal (a plant which lacks stomata) to test assumptions linked to the Farquhar model of discrimination. This astomatal mutant differs from other naturally occurring astomatal plants such as some species of bryophytes (e.g. *Marchantia polymorpha*) which whilst lacking a stomatal pore and accompanying guard cells have permanently open pores, allowing free exchange of CO_2 between the atmosphere and the plant. Whilst many more species of bryophyte lack fixed pores with CO_2 diffusing across the cell membrane. Consequently the $\Delta^{13}\text{C}$ signature of bryophytes has been used as the basis of the CO_2 proxy, BRYOCARB (Fletcher et al., 2005; 2006). This is because the confounding effects of the isolation of the sub stomatal cavity via the opening and closure of the guard cell system are eliminated. As bryophytes lack a cuticle diffusion of CO_2 through to the site of fixation should also be less limited when compared to vascular plants that have a cuticle. Diffusion will also be affected by the greater distance that CO_2 has to travel to the site of fixation in vascular plants when compared to non-vascular plants. Consequently we hypothesize that within the astomatal mutant calculated C_i/C_a (as a reflection of stomatal closure over the life time of leaf growth) should be close to zero reflecting, what is effectively a partially closed system.

2. METHODS

2.1. Plant growth experiments (University of Sheffield)

Seeds of *Arabidopsis thaliana* (ecotype Col-0) were sown onto multipurpose compost (Arthur Bowyers, UK) covered with plastic film and stratified for 3 days at 4°C . They were transferred into growth cabinets (Sanyo-Fitotron Model: SGC097.PPX.F, UK) and grown under a day/night regime of 8/16 h at 25/21 $^\circ\text{C}$ and 55% RH. Light levels during daylight hours were $230 \mu\text{mol m}^{-2} \text{s}^{-1}$. Six separate CO_2 experiments were conducted, with CO_2 held at concentrations of 380, 760, 1000, 1500, 2000 and 3000 ppm with the $\delta^{13}\text{C}_a$ signature becoming more negative as CO_2 increases. Nested within each CO_2 treatment, plants were also subjected to one of three watering regimes; a low water treatment ($10 \text{ ml}^{-1} \text{ day}^{-1}$ 7 cm (diameter) pot $^{-1}$), a medium water treatment ($20 \text{ ml}^{-1} \text{ day}^{-1}$ 7 cm (diameter) pot $^{-1}$) or high water treatment (consistently saturated compost) imposed after 4 weeks of growth. Following the imposition of water

treatment, plants were left to develop for a further 2 weeks and leaves that had developed under each treatment were subsequently harvested for carbon isotope ratio analysis. Specifically to test for an isotopic effect within the 3000 ppm experiment we grew the astomatal mutant, Hamlet and its associated wild type, to test for variations in calculated C_i/C_a .

2.2. Plant growth experiments (University of Nottingham)

In Nottingham seeds of *A. thaliana* (ecotype, Ler 0, Col-1 and Wa-1) were treated as above but grown in Levington M3 compost. Plants were placed into one of two controlled environment walk-in growth rooms (Unigrow, UK) and grown under a day/night regime of 10 h of light per day in a simulated day/night program. Light levels during daylight hours were $300 \mu\text{mol m}^{-2} \text{s}^{-1}$. Night temperature was set at a high of 17°C and daytime temperature peaked at 20°C . Relative humidity was set at 70% CO_2 was set to at 400 ppm in one chamber and at 1200 ppm in the other. Within each CO_2 treatment replicate plants were subjected to one of three water treatments ($10 \text{ ml}^{-1} \text{ day}^{-1}$ 6.5 cm (diameter) pot^{-1} , $20 \text{ ml}^{-1} \text{ day}^{-1}$ cm (diameter) pot^{-1} or permanently saturated).

2.3. Carbon isotope analysis (University of Sheffield)

Five plants per treatment were analysed. Leaves were dried for one week at 70°C and 0.1 mg of plant material per plant was homogenised in a pestle and mortar for analysis. Measurements were made using an ANCA GSL preparation module, coupled to a 20–20 stable isotope mass spectrometer (PDZ Europa, Cheshire, U.K.). The isotope values for $\delta^{13}\text{C}$ are reported as per mil (‰) deviations of the isotopic ratios ($^{13}\text{C}/^{12}\text{C}$) calculated to the VPDB scale using within-run laboratory working standards calibrated against IAEA-CH-6. Replicate analysis indicated a precision of $\pm 0.15\%$. Air samples from growth cabinets were pumped into 10 ml evacuated gas tight vials (Labco Extainer Vials, Labco Ltd, UK) and analysed on the same mass spectrometer.

2.4. Carbon isotope analysis (British Geological Survey)

Plant material grown at the University of Nottingham was analysed at the British Geological Survey. Plant $\delta^{13}\text{C}$ analyses were performed by combustion in a Costech Elemental Analyser (EA) on-line to a VG TripleTrap and Optima dual-inlet mass spectrometer, with $\delta^{13}\text{C}$ values calculated to the VPDB scale using a within-run laboratory standards calibrated against NBS18, NBS-19 and NBS 22. Replicate analysis of well-mixed samples indicated a precision of $+0.1\%$ (1 SD). For ^{13}C analysis of the CO_2 , the gas was first separated from water vapour using a vacuum line. Measurements were made on an Isoprime dual inlet mass spectrometer. The evolved CO_2 was passed over a water trap prior to the mass spectrometer. Isotope values (^{13}C , and ^{18}O not used) are reported as per mil (‰) deviations of the isotopic ratios ($^{13}\text{C}/^{12}\text{C}$, $^{18}\text{O}/^{16}\text{O}$) calculated to the VPDB scale using a within-run laboratory

standard calibrated against NBS-19. Craig correction is also applied to account for ^{17}O . Analytical reproducibility of the standard calcite (KCM) is $<0.1\%$ for $\delta^{13}\text{C}$.

Discrimination, $\Delta^{13}\text{C}$ which is a proxy measure of integrated WUE (WUE_i) over the lifetime of a leaf is calculated as:

$$\Delta^{13}\text{C} = (\delta^{13}\text{C}_a - \delta^{13}\text{C}_p)/(1 + \delta^{13}\text{C}_p/1000) \quad (1)$$

Calculated C_i/C_a , is given by:

$$C_i/C_a = (\delta^{13}\text{C}_a - \delta^{13}\text{C}_p - a)/(b/a) \quad (2)$$

where $\delta^{13}\text{C}_a$ is the carbon isotopic composition of the CO_2 inside the growth cabinet and $\delta^{13}\text{C}_p$ is the carbon isotopic composition of the leaf material, and a and b are constants linked to discrimination (a is discrimination limited by diffusion = 4% and b is the discrimination limited by Rubisco which can vary between 26 and 30% (Farquhar et al., 1980)).

2.5. Statistical analysis

All data analysis was carried out in R v. 3.4.2 (R Core Team, 2017) using the package Rsolnp v. 1.16 (Ghalanos and Theussl, 2015). We generated CO_2 predictions from our $\Delta^{13}\text{C}$ data using the hyperbolic relationship developed by Schubert and Jähren (2012):

$$\Delta^{13}\text{C} = [(A)(B)(\text{CO}_2 + C)]/[A + (B)(\text{CO}_2 + C)] \quad (3)$$

where the asymptote A is equivalent to the maximum rubisco fractionation value, b , in Eq. (2) (Schubert and Jähren, 2012). While A can therefore vary between 26 and 30, Schubert and Jähren (2012) found the best fitting curve had $A = 28.26$, and this value has been used in subsequent papers (Schubert and Jähren, 2013, 2015; Cui and Schubert, 2016, 2017). B and C have been determined by iterative curve fitting, with the most recent formulation of the model having values of $B = 0.22$ and $C = 23.85$ (Cui and Schubert, 2016). We therefore used these A , B , and C values for predicting CO_2 from our $\Delta^{13}\text{C}$ data. We used the one sample Wilcoxon signed rank test to test for significant differences between predicted and growth CO_2 , since this is a non-parametric test and it does not assume normally distributed data (Crawley, 2005). Similarly, we used the Kruskal-Wallis test (Hammer and Harper, 2006) to test between differences in predicted CO_2 among water treatment levels, within each growth CO_2 level.

In addition to using the model parameters derived by Cui and Schubert (2016), we fitted three new curves to our data, one for each water treatment level. We maintained a similar approach to Schubert and Jähren (2012), using Eq. (3) to model the relationship between $\Delta^{13}\text{C}$ and CO_2 subject to the constraint that $\Delta^{13}\text{C} = +4.4\%$ when $\text{CO}_2 = 0$ ppm. The curves were optimised by minimising the root mean squared error (RMSE), using the function “solnp” in the R package Rsolnp (Ghalanos and Theussl, 2015). Following Cui and Schubert (2016) confidence intervals were estimated for the model parameters via bootstrapping. Briefly, the residuals from the fitted curves were resampled with replacement and added back to the model $\Delta^{13}\text{C}$ estimates to create a new pseudo-dataset, the curve

refitted and the new values of A, B and C recorded. This process was repeated 10,000 times to create a distribution of model parameter values, and the 16% and 84% quantiles used to construct 68% confidence intervals.

We explored uncertainty in the CO₂ predictions by performing Monte Carlo error propagation (Cui and Schubert, 2016). To simulate a mixed sedimentary deposit, we bootstrapped (i.e., resampled with replacement) the $\Delta^{13}\text{C}$ values within each growth CO₂ treatment and then calculated the mean within-treatment values. This process was repeated 10,000 times to generate a sampling distribution for each CO₂ level, the means and standard deviations of which were used in the Monte Carlo resampling. Following Cui and Schubert (2016) we kept A fixed at 28.26, with B being normally distributed with a mean of 0.22 and a standard deviation of 0.028. For each randomly chosen B value, C was calculated as $C = [4.4 \times (A)] / [(A - 4.4) \times (B)]$ (Cui and Schubert, 2016). We calculated 10,000 CO₂ values for each CO₂ treatment level using Eq. (3) and 10,000 random draws from the model parameter distributions. As the $\Delta^{13}\text{C}$ value approaches and then exceeds the value of A (here 28.26) CO₂ becomes inestimable by the model: CO₂ estimates derived from $\Delta^{13}\text{C}$ values just below A will exceed 106 ppm; at $\Delta^{13}\text{C}$ values $\geq A$ estimated CO₂ becomes negative (this switch from positive to negative CO₂ estimates, rather than ever increasing positive CO₂ estimates, is due to the hyperbolic relationship used in the model; see Cui and Schubert, 2016 for details). Following Cui and Schubert (2016) we therefore discarded any CO₂ estimates < 0 and $> 10^6$ ppm. Here, ten estimated CO₂ values were discarded for having a prediction of < 0 ppm.

While Schubert and Jahren (2012) developed Eq. (3) from controlled growth experiments, palaeo-CO₂ reconstructions have been carried out relative to Holocene $\Delta^{13}\text{C}$ and $p\text{CO}_2$ (Schubert and Jahren, 2015; Cui and Schubert, 2016). We followed this approach to test the impact on predicted CO₂ calculated from our $\Delta^{13}\text{C}$ data. Incorporation of Holocene baseline data adds three additional terms to the Monte Carlo error propagation: $\delta^{13}\text{C}_{a(t=0)}$, $\delta^{13}\text{C}_{p(t=0)}$, and $p\text{CO}_{2(t=0)}$. We used the same normal distribution parameters as Cui and Schubert (2016), with $\delta^{13}\text{C}_{a(t=0)} = -6.4\text{‰} \pm 0.1\text{‰}$, $\delta^{13}\text{C}_{p(t=0)} = -25.1\text{‰} \pm 1.6\text{‰}$, and $p\text{CO}_{2(t=0)} = 270 \text{ ppm} \pm 7 \text{ ppm}$ (all uncertainties given as 1 standard deviation); all other terms were resampled as described previously. As before we generated 10,000 CO₂ values for each growth CO₂ treatment level. 6063 results were discarded for having a prediction of < 0 and 12 were discarded for predicting CO₂ $> 10^6$ ppm.

3. RESULTS

Our data demonstrates considerable spread in $\Delta^{13}\text{C}$ within each CO₂ treatment as a function of watering regime (Fig. 2) suggesting that other factors not previously investigated in the context of the C3 plant proxy (Schubert and Jahren, 2012) have the potential to influence estimates of CO₂ based on $\Delta^{13}\text{C}$. To test the assertion that changes in carbon isotope fractionation (*S*) are proportionate to changes in CO₂ and that this is the main factor that drives this relationship, three separate curves of $\Delta^{13}\text{C}$ from the

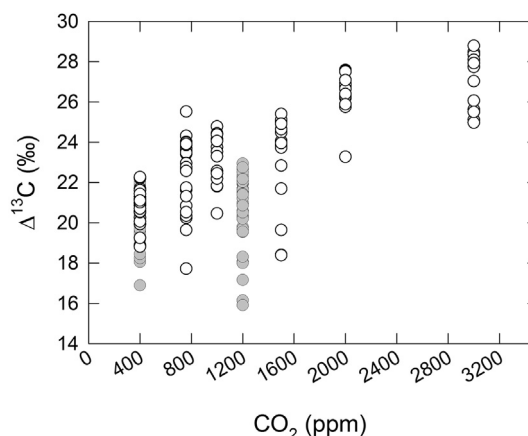


Fig. 2. $\Delta^{13}\text{C}$ values plotted against growth CO₂. Open circles are from plants grown in Sheffield; grey circles are from plants grown in Nottingham.

Sheffield and Nottingham experimental dataset were developed and the difference between and these experiments and the original *A. thaliana* data set of Cui and Schubert (2016) were tested (Fig. 3). Comparison between our water availability treatments shows differences are apparent particularly when comparing the low water treatment (Fig. 3a) to the other water treatments. The 68% confidence interval on the A value for the 10 ml water treatment ($A = 24.44 + 1.78/-1.17$) does not incorporate the A values for the 20 ml ($A = 27.35$) or saturated ($A = 27.48$) water treatments, and the curve for the 10 ml water treatment also has the highest RMSE (Table 1). There are also differences when comparing our datasets to the proposed model (red lines in Fig. 3) of Cui and Schubert (2016). Again, this is most pronounced in the 10 ml water treatment, where the 68% confidence interval on the A value does not overlap with the 28.26 value used by Schubert and Jahren (2012) and Cui and Schubert (2016).

In an attempt to validate the current $\Delta^{13}\text{C}$ C3 proxy we have used the regression of Cui and Schubert (2016) to predict $p\text{CO}_2$ and compared these predicted values to the known CO₂ within the chamber (Fig. 4a). Our data show large differences between predicted and measured growth CO₂ when plants are sampled as individuals, with this variation increasing as atmospheric CO₂ in the chamber increases, with the problem becoming particularly apparent in the 3000 ppm experiment with predictions spanning a CO₂ range of ~ 950 –21,680 ppm. Grouping the data via CO₂ treatment (Fig. 4b) and comparing median CO₂ predictions to growth conditions is analogous to the generation of a $\Delta^{13}\text{C}$ signal from allochthonous deposit that captures material from a broad range of environments. Again the data shows a consistent under prediction in CO₂ when the median predicted CO₂ is compared to growth conditions with significant differences in the 380 (Wilcoxon $W = 75$, $n = 29$, $p = 0.0014$), 400 (Wilcoxon $W = 135$, $n = 42$, $p = 2.94 \times 10^{-5}$), 760 ($W = 23$, $n = 29$, $p = 2.38 \times 10^{-6}$), 1000 ($W = 0$, $n = 14$, $p = 0.0001$), 1200 ($W = 0$, $n = 43$, $p = 2.27 \times 10^{-13}$) and 1500 ($W = 0$,

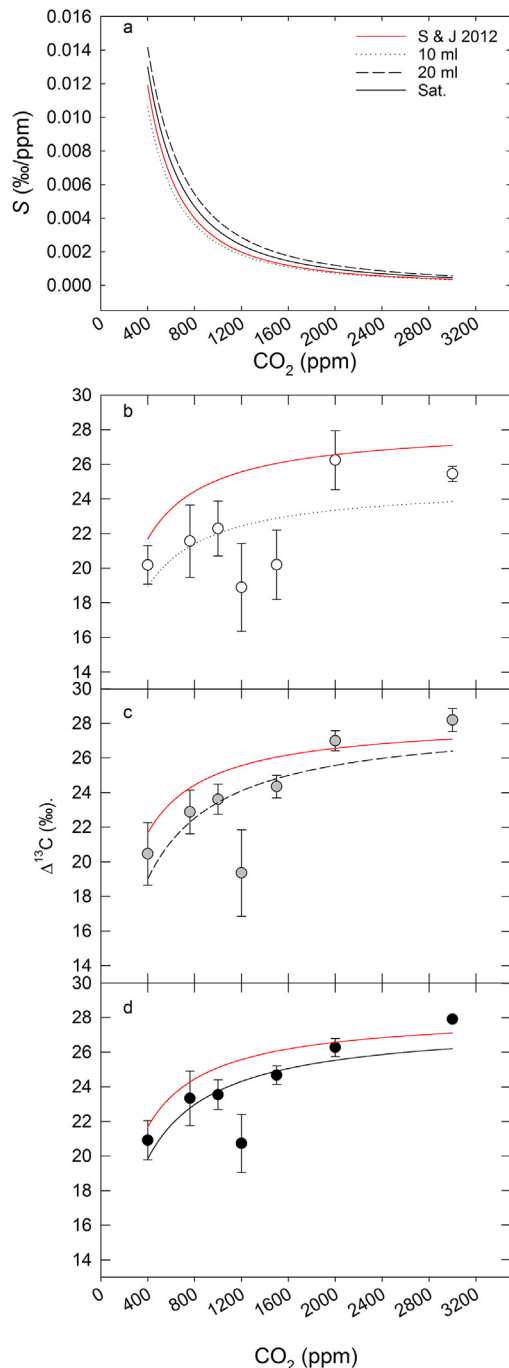


Fig. 3. Change in $\Delta^{13}\text{C}$ plotted against atmosphere CO_2 . a, change in $\Delta^{13}\text{C}$ per ppm of CO_2 (S) calculation is based on Cui and Schubert (2016) and compares work presented in this study to that of Cui and Schubert (2016); b, change in $\Delta^{13}\text{C}$ per ppm of CO_2 for plants grown in the low water treatment (10 ml), dotted line is the curve fit for this dataset based on the protocol of Cui and Schubert (2016); c, change in $\Delta^{13}\text{C}$ per ppm of CO_2 for plants grown in the moderate water treatment (20 ml), dashed line is the curve fit as per Cui and Schubert (2016) and d, change in $\Delta^{13}\text{C}$ per ppm of CO_2 for plants grown in the high water treatment (Sat), solid line is the curve fit for this dataset as per Cui and Schubert (2016). The red line in panel b–d is the curve fit from Cui and Schubert (2016). (For interpretation of the references to colour in this figure legend, the reader is referred to the web version of this article.)

$n = 15$, $p = 0.0001$) ppm CO_2 treatments (a full statistical break down of results is given in the [supplementary information](#)). Breaking the data down to evaluate how different watering treatments effect the utility of $\Delta^{13}\text{C}$ reveals the lack of a systematic signal with water treatment (Fig. 5). While the 10 ml treatment level typically leads to lower CO_2 estimates, the pattern is not consistent between the 20 ml and saturated treatments. There are statistically significant differences among water treatment levels at the 380 (Kruskal-Wallis $H = 7.19$, $p = 0.03$), 760 ($H = 6.38$, $p = 0.04$), 1200 ($H = 14.09$, $p = 0.001$), 1500 ($H = 9.62$, $p = 0.008$) and 3000 ($H = 7.36$, $p = 0.03$) ppm CO_2 treatment levels, and a full statistical break down of results is in the [supplementary information](#).

While A has been fixed at 28.26 for previous proxy development and applications (Schubert and Jahren, 2012, 2013, 2015; Cui and Schubert, 2016, 2017), Cui and Schubert (2016) considered the impact of varying A from 26 to 30, with B and C changing accordingly. To test if other values of A , B and C would produce more accurate CO_2 estimates relative to the growth conditions we used the alternative values provided by Cui and Schubert (2016) (Table 2). Comparing both the r^2 values from regressions of estimated on growth CO_2 and root mean squared error of prediction (RMSEP) shows that the most accurate CO_2 reconstructions are found with $A = 30$, which is in agreement with Cui and Schubert (2016). However, even $A = 30$ only yields an r^2 value of 0.57 and a RMSEP of 824 ppm, with underestimation at all CO_2 treatment levels (a full graphical display of predicted CO_2 when A is varied is presented in [appendix B in the supplementary information](#)).

Monte Carlo error propagation using Eq. (3) shows a variety of responses (Fig. 6), but with underestimation of CO_2 at all treatment levels ≤ 1500 ppm. When the full error propagation relative to the Holocene baseline data is carried out the median CO_2 estimates are similar to those derived from Monte Carlo error propagation using Eq. (3), but the spread of the distributions is much larger. This leads to a greater overlap with growth CO_2 conditions but also a greater proportion of unrealistically high CO_2 estimates (Fig. 6).

$\Delta^{13}\text{C}$ for the Hamlet wild type (grown at 3000 ppm) is 30.11 ± 0.13 (1 Standard Deviation). Using $\delta^{13}\text{C}_a$ and $\delta^{13}\text{C}_p$ to calculate C_i/C_a for both the Hamlet mutant and its wild type parent shows that a realistic C_i/C_a is only achievable in the wild type if Rubisco limited discrimination (b) > 29 . When b is set to range between 26.00 and 28.25‰, C_i/C_a is > 1 which from an ecophysiological standpoint is impossible. Analysis of the astomatal mutant Hamlet shows that the $\Delta^{13}\text{C}$ for the mutant is 13.56 ± 0.22 (1 Standard Deviation) and reveals that when b is set at 29 average C_i/C_a is 0.347 and 0.334 when b is set at 30 (Fig. 7). These C_i/C_a values reflect a relatively high internal CO_2 concentration which is incongruent with the astomatal nature of the plant and the low discrimination value which signifies a high WUE and “stomatal” closure as expected in an astomatal plant. It is also plausible that the $\delta^{13}\text{C}_p$ value of the Hamlet leaf tissue could indicate recycling of internal CO_2 .

Table 1

A, B and C values for curves fitted to our data. Numbers in parentheses are bootstrapped 68% confidence intervals, RMSE = root mean squared error.

Water treatment	A	B	C	RMSE
10 ml	24.44 (+1.78/−1.17)	0.25 (+0.17/−0.10)	21.63 (+13.27/−8.97)	1.94
20 ml	27.35 (+1.52/−1.24)	0.19 (+0.08/−0.05)	27.73 (+10.09/−7.84)	1.72
Saturated	27.48 (+1.05/−0.99)	0.19 (+0.05/−0.04)	28.18 (+7.08/−6.15)	1.23

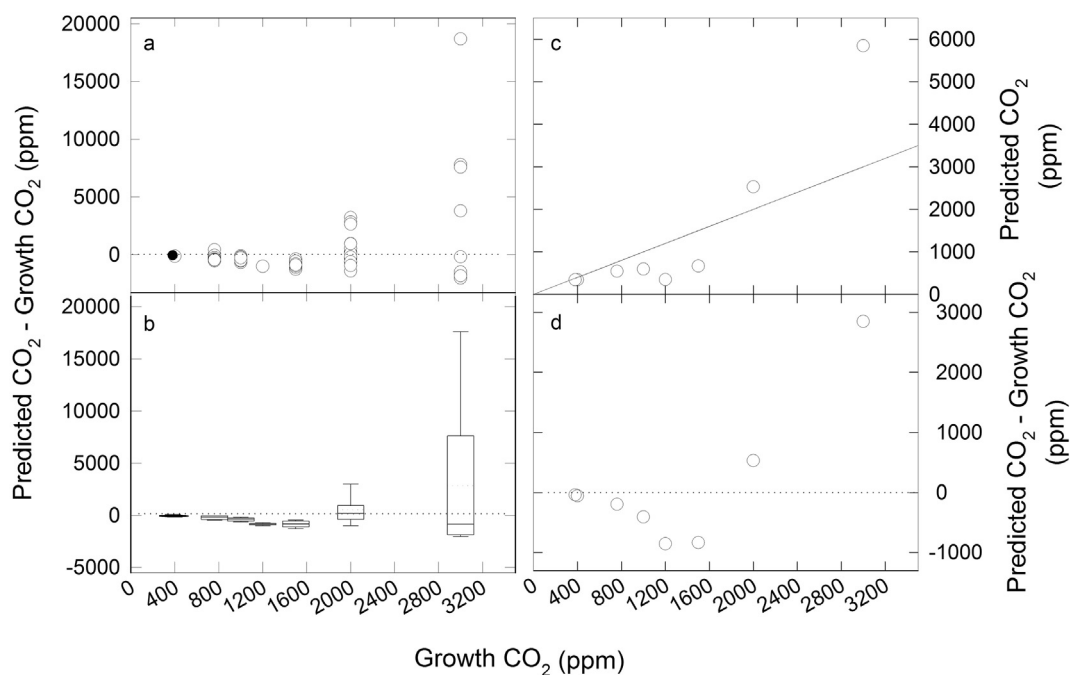


Fig. 4. Comparison between predicted and measured (growth) CO₂ concentrations. a, shows individual data points for each experimental treatment; b, shows these data points plotted collectively as box plots analogous to a fossil sample collected from an assemblage composed of a transported flora (an allochthonous deposit); c, shows the average predicted CO₂ for each CO₂ experiment and the solid black line represents the one to one line; and d, is the average difference between predicted and measured CO₂.

4. DISCUSSION

Our analysis shows that there are clear and consistent impacts of water treatment on the leaf tissue $\delta^{13}\text{C}$, these then obviously feed forward and impact on the utility of the proxy to predict CO₂. It is particularly clear that the 10 ml treatment (low water availability) diverges from predictions made based on the Schubert and Jahren (2012) model resulting in an underestimation in CO₂. It should be noted that in their original publication (Schubert and Jahren, 2012), the authors did state that water availability might be an important factor in their analysis. They consequently suggested that sampling be limited to sites with mean annual precipitation of >2100 mm, which in the modern world are limited to tropical and subtropical environments with consistently high water availability (Wilf et al., 1998; Jaramillo and Cárdenas, 2013). However, in subsequent analysis this caveat seems to have been disregarded with samples being taken from a number of non-tropical locations. Cui and Schubert (2017) do however suggest that mixed/reduced moisture signals might be

a reason for a possible underestimation of their predicted CO₂ through Cenozoic hyperthermal events.

Analysis of our validation data shows a distinct pattern with a general underestimate in predicted CO₂ when compared to growth CO₂ up to atmospheric concentrations of 1500 ppm. This appears to be independent of water treatment. These data are of relevance to Mesozoic (Barral et al., 2017) and Cenozoic (Cui and Schubert, 2017) CO₂ reconstructions as two recent studies using this technique have predicted what could be regarded as anomalously low palaeo-CO₂ particularly through the Cretaceous with estimates as low as ~280 ppm (Barral et al., 2017). If the C3 proxy systematically under predicts CO₂ across this range of CO₂ this may go some way to explaining these CO₂ predictions. It is well known that changes in salinity can affect *WUE* (Guy et al., 1980) so the deltaic/estuarine setting of these plant fossils (Barral et al., 2017) may further influence their $\delta^{13}\text{C}$ composition. This would decouple the $\delta^{13}\text{C}$ signature from the atmosphere further limiting the potential of the $\Delta^{13}\text{C}$ of these plants to be used to predict CO₂ even when the issues raised in our validation

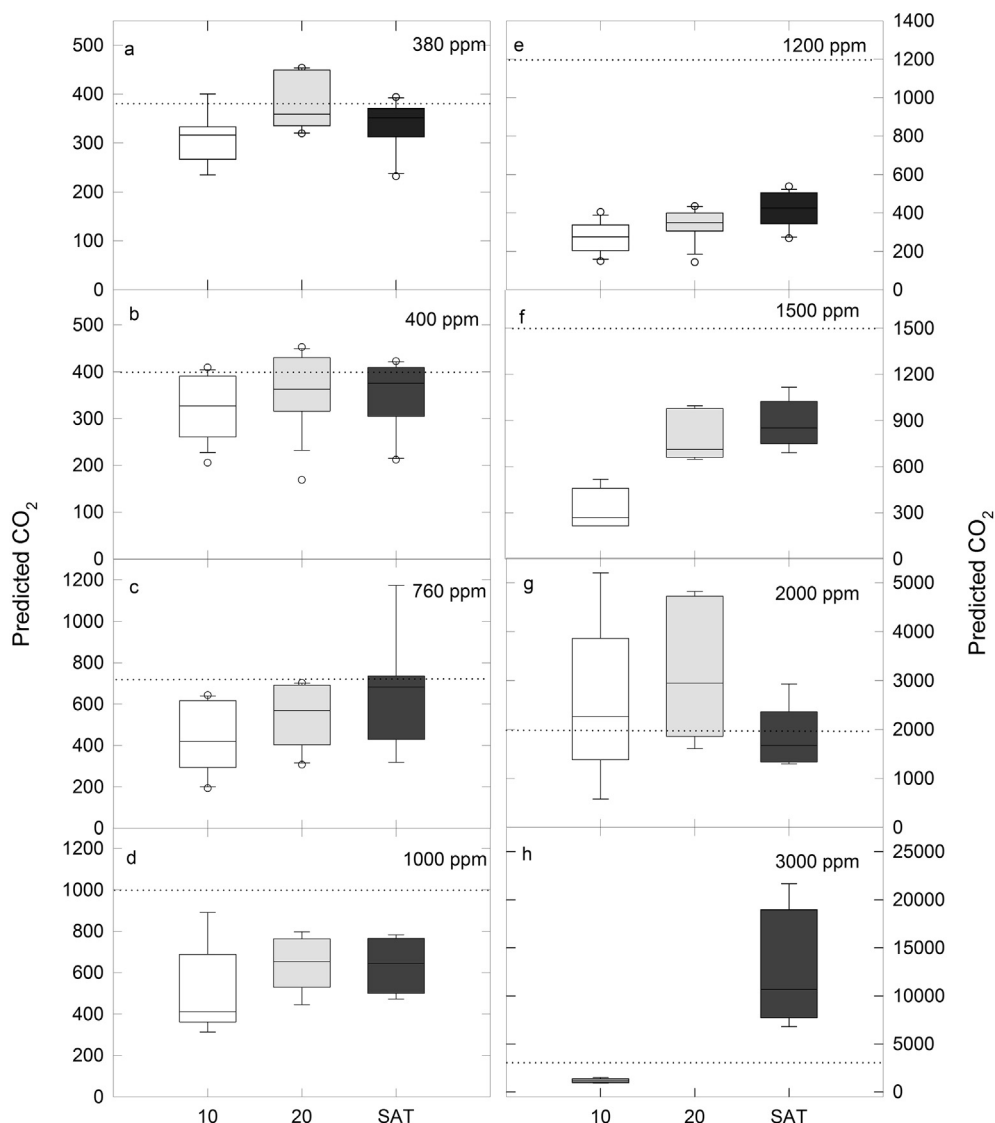


Fig. 5. Box plots comparisons of Sheffield and Nottingham data between predicted and measured (growth) CO_2 concentrations, displayed by water variation in each experimental CO_2 treatment. Note there are statistically significant differences among water treatment levels at the 400, 760, 1200, 1500 and 3000 ppm CO_2 treatment levels, see [Table A2 in supplementary](#) for full a statistical breakdown of our data. Growth CO_2 concentrations are displayed within each panel. Note in there is no box plot for the 20 ml treatment in the 3000 ppm experiment (panel h) as $\Delta^{13}\text{C}$ was greater than A for four of the five replicates predicted CO_2 from the one remaining data point was 2973 ppm. For these calculations of $p\text{CO}_2$ A was set at 28.26 as per [Cui and Schubert \(2016\)](#). A full presentation of CO_2 predictions when A is varied is presented in the [appendix B in supplementary](#).

Table 2
 r^2 values from regressions of estimated on growth CO_2 and root mean squared error of prediction (RMSEP), using A, B and C values provided in [Cui and Schubert \(2016\)](#).

A	B	C	r^2	RMSEP
26	0.16	32.88	0.19	2989.22
27	0.19	28.40	0.13	3128.81
28	0.21	24.70	0.19	4887.09
28.26	0.22	23.85	0.30	1712.87
29	0.24	21.68	0.31	1210.11
30	0.27	19.20	0.57	823.56

assessment are excluded. This combination of factors most likely explains why the majority of the [Barral et al. \(2017\)](#) data plot outside of the 95% confidence limits of the [Foster et al. \(2017\)](#) compilation ([Fig. 1](#)) and are anomalous when compared to stomatal based estimates of CO_2 through the Cretaceous (e.g. [Barclay et al., 2010](#), [Richey et al., 2018](#)).

Our attempt to validate the methodology developed by [Schubert and Jahren \(2012\)](#) and subsequently expanded on by [Cui and Schubert \(2016\)](#) highlights the need to develop validation protocols that allow for the rigorous testing of new proxies ([Jardine and Lomax, 2017](#)). These validation protocols should ideally be based on

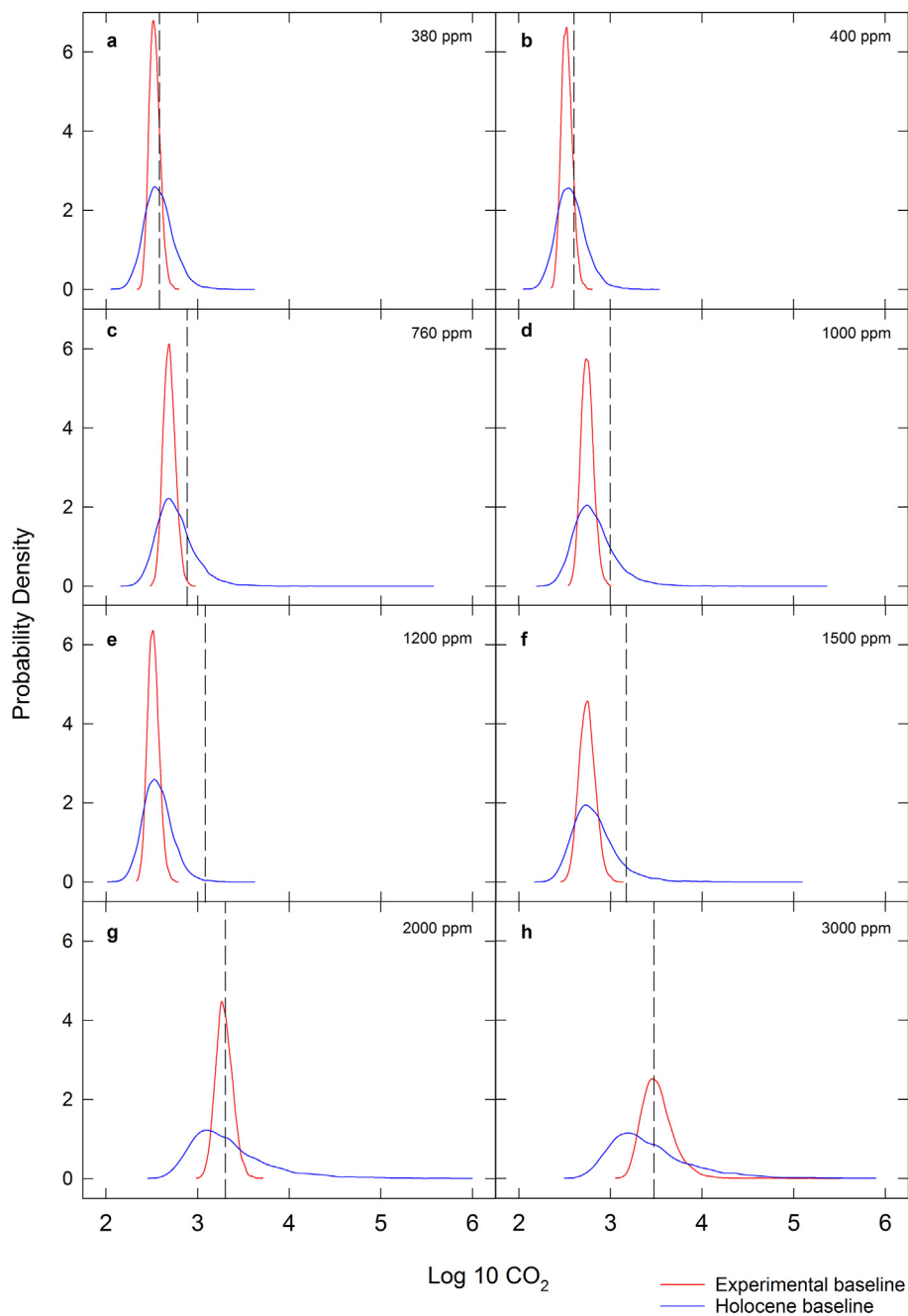


Fig. 6. Probability density function plots of Monte Carlo error propagation. The dotted line represents the log 10 of growth cabinet CO₂; the blue line follows the Holocene protocol and the red line is based solely on our experimental dataset. Growth CO₂ concentrations are displayed within each panel. (For interpretation of the references to colour in this figure legend, the reader is referred to the web version of this article.)

independent data sets or via the segmentation of the original data set, where a proportion of the data set is held back for validation. At the very least cross validation approaches, where each sample (or group of samples) is held back in turn and the value(s) predicted based on the model fit to the rest of the dataset, allow for predictive accuracy to be assessed. However, it should be noted that this type of approach tends to be too optimistic when compared to independent methods of model validation (Zimmermann et al., 2016; Mac Nally et al., 2017). Prior

to our analysis, C3 proxy validation has only been attempted in a geological setting with Schubert and Jahren (2015) demonstrating a close relationship between ice core CO₂ records and their CO₂ reconstructions. However, subsequent work (Kohn, 2016) suggests close agreement might be related to changes in the abundance of C3/C4 grasses that influence the $\delta^{13}\text{C}$ record and are largely independent of atmospheric CO₂ concentration. The lack of congruence in our experimental approach to validation lends supports the interpretation of Kohn (2016).

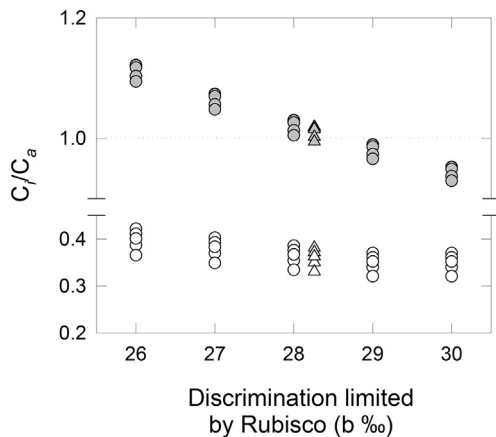


Fig. 7. Calculated changes in C_i/C_a of the astomatal mutant Hamlet and its wild-type parent. Values in C_i/C_a were calculated by changes in values in isotopic discrimination driven by rubisco (b). Grey symbols are the wild type and (Col 0) and open symbols are for the astomatal mutant Hamlet. Triangles show the preferred A value (28.26).

Analysis, via error propagation (Cui and Schubert, 2016; Schubert and Jahren, 2018) whilst informing on the precision of the predictions, is of limited use in assessing the accuracy of the proxy which underpins the model's utility. This is particularly problematic when the response variable, in this case $\Delta^{13}\text{C}$, is known to be sensitive to a large number of environmental stimuli (as discussed above) which are excluded from parameterisation. For example in the initial study of Schubert and Jahren (2012) all variations in $\Delta^{13}\text{C}$ were assumed to be driven solely by changes in CO_2 despite the well-known effects of water availability and temperature on $\Delta^{13}\text{C}$ all of which could have varied considerably in the experimental setup of Schubert and Jahren (2012).

The model initially proposed by Schubert and Jahren (2012) and then developed by Cui and Schubert (2016) is heavily dependent on some baseline assumption(s). For example it is not possible for the model to predict palaeo- CO_2 if the $\Delta^{13}\text{C}$ values are greater than A . Using the preferred A value of 28.26 within our experimental dataset this situation occurs nine times, all within the 3000 ppm experiment (four incidences occurring in Col 0 and the remainder in the Hamlet wild type). These findings indicate that the original C3 proxy model (equation (3)) fails to adequately describe the underlying ecophysiological processes that drive changes in $\delta^{13}\text{C}_p$ that feed through to drive $\Delta^{13}\text{C}$ which are then used to calculate palaeo- CO_2 . If a lower value of A is prescribed this problem is increased. Consequently environmental conditions which result in high levels of discrimination (high $\Delta^{13}\text{C}$) are unlikely to be suitable for this proxy. In the modern world high $\Delta^{13}\text{C}$ values are associated with plants with open stomata that are typically not water limited, and given the well-known wetland mega bias (Spicer, 1981) in the plant fossil record the sensitivity to high values of A could be problematic. The lack of suitability also raises philosophical questions about the utility of the approach as the original model is only operable over a limited climate space.

Porter et al. (2017) used isotope data to calculate C_i/C_a and compared these calculated values to measured values of C_i/C_a derived from infrared gas exchange (IRGA) data. The difference between these two C_i/C_a values was then used to estimate b (Rubisco limited diffusion) which equates to A in the C3 proxy model of Schubert and Jahren (2012) (presented as Eq. (3) in this study). Porter et al. (2017) worked on a phylogenetically broad range of plants relevant to the fossil record and found that the best estimate of b , as defined by providing the closest fit between measured and calculated C_i/C_a was 27. Using the b value of 28.26 preferred by Schubert and Jahren (2012), Porter et al. (2017) found an under estimate of 5% when comparing calculated to measured C_i/C_a . Within their experimental system Porter et al. (2017) also found that a b value of ≥ 28.26 did not lead to a $C_i > C_a$ when CO_2 was elevated, a finding replicated in our data and leading them to suggest that other factors besides b might influence measured $C_i > C_a$. Porter et al. (2017) demonstrate that “measured C_i/C_a varies with CO_2 , and with differing relationships by plant group indicating that to calculate C_i/C_a in response to changes in CO_2 b should not be a fixed value” as previously suggested (e.g. Gröcke, 2002). Consequently, the fixing of A (in Eq. (3)) at 28.26 as per Schubert and Jahren (2012) is likely to lead to problems when predicting $p\text{CO}_2$.

Our experiments, like those of Schubert and Jahren (2012) and the work of others (e.g. Fletcher et al., 2008; Porter et al., 2017) that were designed to investigate plant responses to elevated CO_2 , have been conducted in growth cabinets where the isotopic signature of the CO_2 is not controlled (i.e. it co-varies with $p\text{CO}_2$) and is highly perturbed when compared to natural settings. Comparison of $\Delta^{13}\text{C}$ and C_i/C_a values of Hamlet and its wild type reveals intriguing and potentially anomalous results. The discrimination value ($\Delta^{13}\text{C}$) indicates, as expected, in an astomatal mutant high WUE suggestive of “stomatal” closure. However values of calculated C_i/C_a indicate a degree of stomatal opening. The experiments we have conducted have been based around the assumption that changes in C_i/C_a as recorded by changes in fractionation ($\Delta^{13}\text{C}$) are to a large extent controlled by changes in stomatal opening as a function of the environment specifically CO_2 and water availability. However, a growing body of ecophysiology literature suggests that this relationship is not quite so straight forward. For example recent work has shown that the isotopic composition of plant material can be altered by a variety of processes that occur after carbon fixation. For example, Busch et al. (2013) demonstrated that C3 plants can fix photorespired and respired CO_2 which feeds through to effect $\Delta^{13}\text{C}$; Lanigan et al. (2008) demonstrated both the effects of photorespiration and carboxylation on $\Delta^{13}\text{C}$; Seibt et al. (2008) looked at the relationship between $\delta^{13}\text{C}_p$ and water use efficiency across a variety of spatial and temporal scales and Cernusak et al. (2009) reviewed six hypotheses relating to patterns of fractionation in C3 plants. Our work on the Hamlet mutant and the anomalous calculated values of C_i/C_a lend support to there being multiple factors that can influence $\delta^{13}\text{C}_p$ which in turn effect $\Delta^{13}\text{C}$ and calculated C_i/C_a .

Alternatively these data could also suggest that changes in the $\delta^{13}\text{C}$ of the CO_2 might be affecting the kinetics of Rubisco discrimination, or that the model used to calculate C_i/C_a breaks down when $\delta^{13}\text{C}_a$ is very negative. Both or either of these factors would thus generate anomalous calculated values in C_i/C_a . Within our experimental system and that of Schubert and Jahren (2012) the concentration of CO_2 and $\delta^{13}\text{C}_a$ are positively correlated. This means that it is impossible to determine if the changes in b which are required to maintain C_i/C_a values that are physiologically possible are driven by the CO_2 concentration or the isotopic value of that CO_2 . If changes in b are underpinned by the $\delta^{13}\text{C}$ of CO_2 rather than the concentration then the reliability of the C3 proxy must be further examined given that $\delta^{13}\text{C}_a$ in experimental systems is very different to the natural atmosphere, as it was in the original study that developed the C3 proxy method. Together these findings suggest that the data suggest that using fossil values of $\Delta^{13}\text{C}$ as a tool to predict palaeo CO_2 should be treated with caution as the factors that govern fractionation and calculated values of C_i/C_a are still not fully understood in living plants. Schubert and Jahren (2018) recently suggested that changes in $\Delta^{13}\text{C}$ in response to elevated CO_2 are mathematically independent of C_i/C_a . In our data analysis we did not consider the effects of photorespiration on our calculated $\Delta^{13}\text{C}$ in different CO_2 growth conditions. However, we have clearly shown that manipulations of water availability alters $\Delta^{13}\text{C}$ when plants are grown together in the same atmospheric conditions (Fig. 3) and this in turn impacts on the predictive ability of changes in $\Delta^{13}\text{C}$ to accurately predict $p\text{CO}_2$.

Over geological time whilst there have been large scale perturbations in the concentration of atmospheric CO_2 the isotopic variation ($\delta^{13}\text{C}_a$) which accompanies this variation in CO_2 is much reduced when compared to experimental systems. This results in a fundamentally different relationship between the experiments and the natural world. To fully disentangle this relationship experiments over a wide CO_2 gradient where $\delta^{13}\text{C}_a$ is kept constant are required. Ideally this experimental programme should be combined with other environmental manipulation that control C_i/C_a and be accompanied by a campaign of IRGA measurements to allow for comparison between measured and calculated C_i/C_a as per Porter et al. (2017).

5. CONCLUSIONS

We have set out to deliver a robust experimental framework to fully explore environmental controls on the carbon isotope discrimination in plants. This was undertaken to try and validate the proposed C3 plant proxy as a tool to predict palaeo- CO_2 . Comparisons between predicted and growth CO_2 concentrations show that the model fails to accurately predict CO_2 with substantial under prediction in CO_2 in experiments that were designed to simulate Cenozoic and Mesozoic atmospheric environments. Our findings suggest serious limitations in the proposed proxy as delivered estimates of CO_2 are neither precise nor accurate when compared to known growth conditions.

ACKNOWLEDGEMENTS

Initial support for this work was through a University of Sheffield Biology Division Small Grant to BHL and JAL. At this time JAL was supported through a Royal Society Dorothy Hodgkin Fellowship, UK, and BHL was funded through a Leverhulme Trust Early Career Fellowship [ECF/2006/0492]. Subsequent work at Nottingham was supported via a NERC New Investigators grant NE/J004855/1 and a NERC Isotope Geosciences Facilities Steering Committee grant [IP-1582-1115] both awarded to BHL. We Thank Prof. Carmen Fenoll (Universidad de Castilla-la Mancha) for supply of Hamlet mutants. We also thank Isabel Montañez, two anonymous reviewers and the Associate Editor Miryam Bar-Matthews for their helpful comments and suggestions that improved this paper.

APPENDIX A. SUPPLEMENTARY MATERIAL

Supplementary data associated with this article can be found, in the online version: Appendix A is a full statistical breakdown of results; Appendix B shows a full graphical representation of predicted $p\text{CO}_2$ with variations in A; Appendix C provides the R code required to run the analysis and Appendix D the $\delta^{13}\text{C}_p$ and $\delta^{13}\text{C}_a$ data. Supplementary data to this article can be found online at <https://doi.org/10.1016/j.gca.2018.12.026>.

REFERENCES

- Barclay R. S., McElwain J. C. and Sageman B. B. (2010) Carbon sequestration activated by a volcanic CO_2 pulse during Ocean Anoxic Event 2. *Nat. Geosci.* **3**, 205–208.
- Barral A., Gomez B., Fourel F., Daviero-Gomez V. and Lécuyer C. (2017) CO_2 and temperature decoupling at the million-year scale during the Cretaceous Greenhouse. *Sci. Rep.* **7**, 8310. <https://doi.org/10.1038/s41598-017-08234-0>.
- Bergman N. M., Lenton T. M. and Watson A. J. (2004) COPSE: a new model of biogeochemical cycling over Phanerozoic time. *Am. J. Sci.* **304**, 397–437.
- Berner R. A. and Kothavala Z. (2001) GEOCARB III: a revised model of atmospheric CO_2 over Phanerozoic time. *Am. J. Sci.* **301**, 182–204.
- Berner R. A. (2006) GEOCARBSULF: a combined model for Phanerozoic atmospheric O_2 and CO_2 . *Geochim. Cosmochim. Acta* **70**, 5653–5664.
- Busch F., Sage T. L., Cousins A. B. and Sage R. F. (2013) C3 plants enhance rates of photosynthesis by reassimilating photorespired and respired CO_2 . *Plant Cell Environ.* **36**, 200–212.
- Cernusak L. A., Tcherkez G., Keitel C., Cornwell W. K., Santiago L. S., Knobl A., Barbour M. M., Williams D. G., Reich P. B., Ellsworth D. S., Dawson T. E., Griffiths H., Farquhar G. D., Wright I. J. and Westoby M. (2009) Within plant variation in stable carbon isotopes: why are non-photosynthetic tissues generally ^{13}C enriched compared to leaves? *Funct. Plant Biol.* **36**, 199–213.
- Cernusak L. A., Ubierna N., Winter K., Holtum J. A. M., Marshall J. D. and Farquhar G. D. (2013) Environmental and physiological determinants of carbon isotope discrimination in terrestrial plants. *New Phytol.* **200**, 950–965.
- Crawley M. J. (2005) *Statistics: An Introduction Using R*. John Wiley & Sons Ltd., Chichester.

- Cui Y. and Schubert B. A. (2016) Quantifying uncertainty of past $p\text{CO}_2$ determined from changes in C3 plant carbon isotope fractionation. *Geochim. Cosmochim. Acta* **172**, 127–138.
- Cui Y. and Schubert B. A. (2017) Atmospheric $p\text{CO}_2$ reconstructed across five early Eocene global warming events. *Earth Planet. Sci. Lett.* **478**, 225–233.
- Diefendorf A. F., Mueller K. E., Wing S. L., Koch P. L. and Freeman K. H. (2010) Global patterns in leaf ^{13}C discrimination and implications for studies of past and future climate. *Proc. Natl. Acad. Sci. U.S.A.* **107**(13), 5738–5743.
- Ehleringer J. R., Field C. B., Lin Z. F. and Kuo C. Y. (1986) Leaf carbon isotope and mineral composition in subtropical plants along an irradiance cline. *Oecologia* **70**, 520–526.
- Farquhar G. D., von Caemmerer S. and Berry J. A. (1980) A biochemical model of photosynthetic CO_2 assimilation in leaves of C3 plants. *Planta* **149**, 78–90.
- Fletcher B. J., Beerling D. J., Brentnall S. J. and Royer D. L. (2005) Fossil bryophytes as recorders of ancient CO_2 levels: experimental evidence and a Cretaceous case study. *Global Biogeochem. Cycles* **19**, GB3012. <https://doi.org/10.1029/2005GB002495>.
- Fletcher B. J., Brentnall S. J., Quick W. P. and Beerling D. J. (2006) BRYOCARB: a process-based model of thallose liverwort carbon isotope fractionation in response to CO_2 , O_2 , light and temperature. *Geochim. Cosmochim. Acta* **70**, 5676–5691.
- Fletcher B. J., Brentnall S. J., Anderson C. W., Berner R. A. and Beerling D. J. (2008) Atmospheric carbon dioxide linked with Mesozoic and early Cenozoic climate change. *Nat. Geosci.* **1**, 43–48.
- Foster G. L., Royer D. L. and Lunt D. J. (2017) Future climate forcing potentially without precedent in the last 420 million years. *Nat. Commun.* **8**, 14845.
- Franks P. J., Royer D. L., Beerling D. J., van de Water P. K., Cantrill D. J., Barbour M. M. and Berry J. A. (2014) New constraints on atmospheric CO_2 concentration for the Phanerozoic. *Geophys. Res. Lett.* **41**, 4685–4694.
- Franks P. J. and Royer D. L. (2017) Comment on “Was atmospheric CO_2 capped at 1000 ppm over the past 300 million years?” by McElwain J. C. et al. [*Palaeogeogr. Palaeoclimatol. Palaeoecol.* **441** (2016) 653–658]. *Palaeogeogr. Palaeoclimatol. Palaeoecol.* **472**, 256–259.
- Ghalanos A. and Theussl S. (2015) Rsolnp: General Non-linear Optimization Using Augmented Lagrange Multiplier Method. R package version 1.16.
- Gröcke D. R. (2002) The carbon isotope composition of ancient CO_2 based on higher-plant organic matter. *Philos. Trans. R. Soc. A.* **360**, 633–658.
- Guy R. D., Reid D. M. and Krouse H. R. (1980) Shifts in carbon isotope ratios of two C3 halophytes under natural and artificial conditions. *Oecologia* **44**, 241–247.
- Hammer Ø. and Harper D. A. T. (2006) *Paleontological Data Analysis*. Blackwell Publishing Ltd., Oxford.
- Jahren A. H. and Arens N. C. (2009) Prediction of atmospheric $\text{d}^{13}\text{C}\text{O}_2$ using plant cuticle isolated from fluvial sediment: tests across a gradient in salt content. *Palaios* **24**, 394–401.
- Jaramillo C. and Cárdenas A. (2013) Global warming and neotropical rainforests: a historical perspective. *Annu. Rev. Earth Planet. Sci.* **41**, 741–766.
- Jardine P. E. and Lomax B. H. (2017) Is pollen size a robust proxy for moisture availability? *Rev. Palaeobot. Palynol.* **246**, 161–166.
- Kohn M. J. (2010) Carbon isotope compositions of terrestrial C3 plants as indicators of (paleo)ecology and (paleo)climate. *Proc. Natl. Acad. Sci. U.S.A.* **107**, 19691–19695.
- Kohn M. J. (2016) Carbon isotope discrimination in C3 land plants is independent of natural variations in $p\text{CO}_2$. *Geochim. Persp. Lett.* **2**, 35–43.
- Körner C., Farquhar G. D. and Wong S. C. (1991) Carbon isotope discrimination by plants follows latitudinal and altitudinal trends. *Oecologia* **88**, 30–40.
- Lanigan G. J., Betson N., Griffiths H. and Seibt U. (2008) Carbon isotope fractionation during photorespiration and carboxylation in *Senecio*. *Plant Physiol.* **148**, 2013–2020.
- Lomax B. H., Knight C. A. and Lake J. A. (2012) An experimental evaluation of the use of C3 $\delta^{13}\text{C}$ plant tissue as a proxy for the paleoatmospheric $\delta^{13}\text{C}\text{CO}_2$ signature of air. *Geochim. Geophys. Geosyst.* **13**, Q0AI03. <https://doi.org/10.1029/2012GC004174>.
- Lomax B. H. and Fraser W. T. (2015) Palaeoproxies: botanical monitors and recorders of atmospheric change. *Palaeontology* **58**, 759–768.
- Mac Nally R., Duncan R. P., Thomson J. R. and Yen J. D. L. (2017) Model selection using information criteria, but is the “best” model any good? *J. Appl. Ecol.* <https://doi.org/10.1111/1365-2664.13060>.
- McElwain J. C., Montañez I. P., White J. D., Wilson J. P. and Yiotis C. (2016) Was atmospheric CO_2 capped at 1000 ppm over the past 300 million years? *Palaeogeogr. Palaeoclimatol. Palaeoecol.* **441**, 653–658.
- McElwain J. C., Montañez I. P., White J. D., Wilson J. P. and Yiotis C. (2017) Reply to comment on “Was atmospheric CO_2 capped at 1000 ppm over the past 300 million years?” [*Palaeogeogr. Palaeoclimatol. Palaeoecol.* **441** (2016) 653–658]. *Palaeogeogr. Palaeoclimatol. Palaeoecol.* **472**, 260–263.
- Morris J., Leake J. R., Stein W. E., Berry C. M., Marshall J. E. A., Wellman C. H., Milton J. A., Hillier S., Mannolini F., Quirk J. and Beerling D. J. (2015) Investigating Devonian trees as geoengineers of past climates: linking palaeosols to palaeobotany and experimental geobiology. *Palaeontology* **58**, 787–801.
- Porter A. S., Yiotis C., Montañez I. P. and McElwain J. C. (2017) Evolutionary differences in $\Delta^{13}\text{C}$ detected between spore and seed bearing plants following exposure to a range of atmospheric O_2/CO_2 ratios; implications for paleoatmosphere reconstruction. *Geochim. Cosmochim. Acta* **213**, 517–533.
- R Core Team (2017) *R: A Language and Environment for Statistical Computing*. R Foundation for Statistical Computing, Vienna, Austria.
- Richey J. D., Upchurch G. R., Montañez I. P., Lomax B. H., Suarez M. B., Crout N. M. J., Joeckele R. M., Ludvigson G. A. and Smith J. J. (2018) Changes in CO_2 during Ocean Anoxic Event 1d indicate similarities to other carbon cycle perturbations. *Earth Planet. Sci. Lett.* **491**, 172–182.
- Royer D. L., Donnadieu Y., Park J., Kowalczyk J. and Goddés Y. (2014) Error analysis of CO_2 and O_2 estimates from the long-term geochemical model GEOCARBSULF. *Am. J. Sci.* **314**, 1259–1283.
- Schleser G. H. (1990) Investigations of the d^{13}C pattern in leaves of *Fagus sylvatica* L.. *J. Ex. Bot.* **41**, 565–572.
- Schubert B. A. and Jahren A. H. (2012) The effect of atmospheric CO_2 concentration on carbon isotope fractionation in C3 land plants. *Geochim. Cosmochim. Acta* **96**, 29–43.
- Schubert B. A. and Jahren A. H. (2013) Reconciliation of marine and terrestrial carbon isotope excursions based on changing atmospheric CO_2 levels. *Nat. Commun.* **4**, 1653. <https://doi.org/10.1038/ncomms2659>.
- Schubert B. A. and Jahren A. H. (2015) Global increase in plant carbon isotope fractionation following the Last Glacial Maximum caused by increase in atmospheric $p\text{CO}_2$. *Geology* **43**, 435–438.

- Schubert B. A. and Jahren A. H. (2018) Incorporating the effects of photosynthesis into terrestrial paleoclimate reconstructions. *Earth Sci. Rev.* **177**, 637–642.
- Seibt U., Rajabi A., Griffiths H. and Berry J. (2008) Carbon isotopes and water use efficiency: sense and sensitivity. *Oecologia* **155**, 441–454.
- Spicer R. A. (1981) The sorting and deposition of allochthonous plant material in a modern environment at Silwood Lake, Silwood Park, Berkshire, England. *US Geol. Surv. Prof. Pap.* **1143**, 1–77.
- Stemans P., Hérisse A. L., Melvin J., Miller M. A., Paris F., Verniers J. and Wellman C. H. (2009) Origin and radiation of the earliest vascular land plants. *Science* **324**, 353.
- Wilf P., Wing S. L., Greenwood D. R. and Greenwood C. L. (1998) Using fossil leaves as paleoprecipitation indicators: an Eocene example. *Geology* **26**, 203–206.
- Zimmermann B., Tafintseva V., Bağcıoğlu M., Høegh Berdahl M. and Kohler A. (2016) Analysis of allergenic pollen by FTIR microspectroscopy. *Anal. Chem.* **88**, 803–811.

Associate editor: Miryam Bar-Matthews